Adaptive Super-Twisting Sliding Mode Fault-Tolerant Control of Launch Vehicles with Actuator Faults

WANG Kejun[1], *ZHOU Zhijie*[1*], *FENG Zhichao*[1], *YANG Ruohan*[2], *HU Changhua*[1], *XU Hui*[1]

1. Rocket Force University of Engineering, Xi'an 710025, P. R. China;
2. College of Electronics and Information, Northwestern Polytechnical University, Xi'an 710129, P. R. China

(Received 20 September 2024; revised 20 November 2024; accepted 30 November 2024)

Abstract: A fault-tolerant control law based on adaptive super-twisting sliding mode control (SMC) is designed for the attitude command tracking problem of a launch vehicle with actuator faults, considering the uncertainties arising from unknown external disturbances, fuel consumption of the launch vehicle, and the perturbation due to the change in rotational inertia caused by tank sloshing, as well as the potential system model changes due to actuator fault and unmodeled dynamics. This control algorithm integrates the super-twisting SMC, the fuzzy logic control, and the adaptive control. First, a super-twisting sliding surface is selected to mitigate the "chattering" phenomenon inherent in SMC, ensuring that the system tracking error converges to zero within a finite time. Second, building upon this sliding surface, the fuzzy logic control is used to approximate the unknown system function, which includes fault information. Adaptive parameters are used to approach the system parameters and enhance disturbance rejection. The stability and finite-time convergence of the launch vehicle attitude tracking control system are verified by the Lyapunov method. Numerical simulations demonstrate the effectiveness and robustness of the proposed adaptive super-twisting SMC algorithm.

Key words: launch vehicle; actuator fault; super-twisting sliding mode control (SMC); fault-tolerant control; fuzzy logic control

CLC number: V249 **Document code:** A **Article ID:** 1005-1120(2024)06-0689-11

0 Introduction

In aerospace science, launch vehicles are key tools for exploring deep space and have become a strategic focus of scientific research and technological advancement for many countries. Examples include NASA's Ares series and China's Long March series[1-3]. These vehicles perform crucial missions such as manned spaceflight, scientific experiments, and satellite deployment. Mission failures can cause substantial economic losses and significantly impact a nation's military strategy and diplomatic standing[4]. Therefore, ensuring the stable and reliable operation of launch vehicles in the complex and dynamic space environment is critical to aerospace engineering.

In control system design, launch vehicles face several technical challenges, including significant external environmental interference, complex and uncertain dynamic models, and potential actuator faults. To address these challenges, an efficient, robust, and highly fault-tolerant flight control system is crucial. This system must ensure reliable launch vehicle flights under various extreme conditions for mission success.

Sliding mode control (SMC), known for its simple implementation, rapid response, and strong robustness, has been widely used in areas such as robot control, chemical process control, and aero-

*Corresponding author, E-mail address: zhouzj04@tsinghua.org.cn.

How to cite this article: WANG Kejun, ZHOU Zhijie, FENG Zhichao, et al. Adaptive super-twisting sliding mode fault-tolerant control of launch vehicles with actuator faults[J]. Transactions of Nanjing University of Aeronautics and Astronautics, 2024, 41(6): 689-699.

http://dx.doi.org/10.16356/j.1005-1120.2024.06.002

space[5-7]. However, SMC has drawbacks. Primarily, it uses a switching term based on a sign function to suppress uncertain disturbances, often requiring a large switching gain to cover the uncertainty boundary. In practical applications, actuators possess system, time, and space inertia, which prevents the system state from strictly moving towards the equilibrium point along the switching surface. This can lead to high-frequency oscillations in the closed-loop system, resulting in chattering. Chattering can significantly impact control accuracy and, in severe cases, even destabilize the system. To mitigate chattering, researchers have developed techniques such as boundary layer control[8] and super-twisting control[9]. Boundary layer control, as described in Ref.[8], uses a saturation function, instead of a sign function, to reduce chattering with compromising robustness, because the system state converges only within the boundary layer. The super-twisting algorithm (STA), a well-known second-order sliding mode algorithm introduced in Ref.[10], hides the high-frequency switching function in the higher-order derivatives of the sliding variable. This causes the switching control law to consider an integral term based on the switching function. Since the integral acts as a filter, it effectively suppresses the "chattering" inherent in SMC[9]. In Ref.[11], a novel adaptive super-twisting global integral terminal sliding mode control algorithm was proposed for trajectory tracking of autonomous robotic manipulators with parametric uncertainties, unknown disturbances, and actuator faults. The system's stability was demonstrated by the Lyapunov method, and simulations confirmed the control scheme's effectiveness. In Ref.[12], an adaptive proportional-integral-derivative (PID) SMC technique, combined with a super-twisting algorithm, was used to stabilize a rotary inverted pendulum under external disturbances. The Lyapunov stability theory verified the system's stability, and simulations provided validation. In Ref.[13], an adaptive gain super-twisting SMC method was employed to address the tracking control problem of an unmanned surface vehicle with twin hulls. This method was verified to have a suitable control performance despite uncertain loads and external disturbances. In Ref.[14], a new type of disturbance observer was combined with super-twisting sliding mode technology to enhance the performance of a permanent magnet synchronous motor speed control system, forming a composite controller with feedforward compensation and state feedback control. This composite controller estimated and compensated for the lumped unknown disturbance. Simulation experiments also fully verified the effectiveness and robustness of the proposed composite control scheme.

This paper introduces an adaptive super-twisting sliding mode nonlinear control law for the attitude control system of a launch vehicle with actuator faults. A key contribution is a novel control scheme with reduced requirements. This is achieved by incorporating the virtual parameter estimation error into the Lyapunov function candidate. This approach eliminates the need for detailed system parameter information for both control design and implementation, which is a significant advantage. The controller strategically focuses on the relationship between the actuator compensation magnitude and the actuator performance, thereby circumventing complex and costly fault detection and identification processes. This directly overcomes the limitation of fault-tolerant control relying on the accuracy of fault diagnosis. Consequently, the proposed controller ensures the same level of precision in both fault and fault-free conditions, demonstrating robustness. Furthermore, the developed method demonstrates rapid responsiveness in the event of abrupt failures, which is a featured advantageous for practical applications and highlights its practical relevance. The main innovations are as follows.

(1) The control law is designed directly for the nonlinear attitude dynamic model of a launch vehicle without the need for linearization of the model.

(2) In the design of the control law, not only unknown external disturbances are considered, but also the perturbation caused by the changes in the moment of inertia due to fuel consumption and tank sloshing of the launch vehicle, as well as the uncertain terms and potential system model changes caused by actuator faults and unmodeled dynamics

present in the model.

(3) SMC has the advantages of rapidity and robustness, but traditional SMC contains a sign function, requiring high-frequency switching of control signals, which not only imposes high hardware requirements but also causes chattering in the system. Super-twisting SMC incorporates integral action to obtain the actual control value, without high-frequency switching, thus avoiding system chattering. Moreover, based on Lyapunov functions, it is proven that the system can reach the sliding surface in finite time and ensure that the tracking error converges to zero along the super-twisting sliding surface in finite time.

(4) The super-twisting sliding mode nonlinear control law, which is applied to single-input single-output systems, is extended to multi-input multi-output systems.

(5) This method primarily uses super-twisting SMC and utilizes fuzzy logic systems to handle unknown functions in the model.

1 Problem Statement and Preliminaries

1.1 Launch vehicle attitude control system model

A large launch vehicle is equipped with eight engines, including four booster engines (actual deflection angles δ_1^z, δ_2^z, δ_3^z, δ_4^z) and four core stage engines (actual deflection angles δ_1^x, δ_2^x, δ_3^x, δ_4^x), as shown in Fig.1. The blue nozzles are fixed nozzles, while the others are deflecting nozzles. The arrow direction indicates the direction of engine deflection. The launch vehicle has a three-channel decoupled control system. R represents the distance from the booster engine to the rocket's central axis and r the distance from the core stage engine to the rocket's central axis.

The relationship between the equivalent deflection angle of the three channels of the launch vehicle and the deflection angles of the booster engines and the core stage engines is

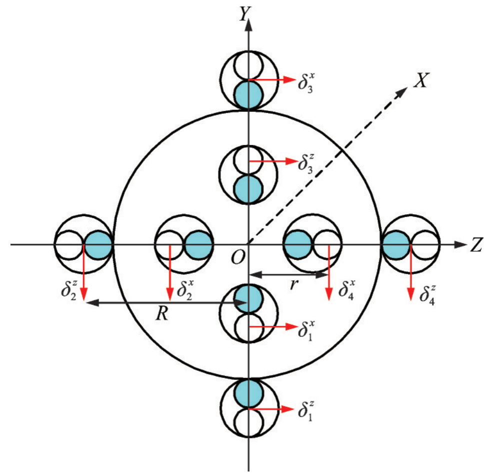

Fig.1 Configuration of rocket engines (view from tail)

$$\boldsymbol{\delta}=\begin{bmatrix}\delta_\phi\\ \delta_\psi\\ \delta_\gamma\end{bmatrix}=\boldsymbol{\delta}^z+\boldsymbol{\delta}^x=\boldsymbol{Q}\left(\begin{bmatrix}\delta_1^x\\ \delta_2^x\\ \delta_3^x\\ \delta_4^x\end{bmatrix}+\begin{bmatrix}\delta_1^z\\ \delta_2^z\\ \delta_3^z\\ \delta_4^z\end{bmatrix}\right) \tag{1}$$

where $\boldsymbol{\delta}^z$ represents the equivalent deflection angle vector of the booster engine and $\boldsymbol{\delta}^x$ the equivalent deflection angle vector of the core stage engine; δ_ϕ, δ_ψ, δ_γ represent the equivalent roll, yaw, and pitch angles of the launch vehicle, respectively, and

$$\boldsymbol{Q}=\begin{bmatrix}-\frac{1}{4} & -\frac{1}{4} & \frac{1}{4} & \frac{1}{4}\\ \frac{1}{2} & 0 & \frac{1}{2} & 0\\ 0 & \frac{1}{2} & 0 & \frac{1}{2}\end{bmatrix}$$

The control torque can be expressed as

$$\boldsymbol{u}=\boldsymbol{B\delta}=-P\mathrm{diag}((4R+2r),\ 3(X_R-X_Z),3(X_R-X_Z)) \tag{2}$$

where $\boldsymbol{B}\in\mathbf{R}^{3\times3}$ is the torque conversion matrix between the equivalent pendulum angle and the control torque; X_R the distance from the engine nozzle to the top of the rocket; X_Z the position of the center of mass; and P the thrust of each engine.

The attitude motion equations of the launch vehicle can be obtained as

$$\dot{\boldsymbol{\Omega}}=Z(\boldsymbol{\Omega})\boldsymbol{\omega}=\begin{bmatrix}1 & \tan\psi\sin\phi & \tan\psi\cos\phi\\ 0 & \cos\phi & -\sin\varphi\\ 0 & \sec\psi\sin\phi & -\sec\psi\cos\phi\end{bmatrix}\boldsymbol{\omega} \tag{3}$$

where $Z(\boldsymbol{\Omega})$ is the coordinate transformation matrix $\boldsymbol{\Omega}=[\phi\quad\psi\quad\gamma]^{\mathrm{T}}\in\mathbf{R}^3$ the attitude angle vector, ϕ the roll angle, ψ the yaw angle, and γ the pitch angle; and $\boldsymbol{\omega}=[\omega_\phi \quad \omega_\psi \quad \omega_\gamma]^{\mathrm{T}}\in\mathbf{R}^3$ the attitude angular velocity vector of the launch vehicle.

For a certain large launch vehicle, by ignoring elastic modes and considering fuel sloshing and aerodynamic torques in the disturbances, its rotational motion model can be represented as[15]

$$\boldsymbol{J}\dot{\boldsymbol{\omega}}=-\begin{bmatrix}0 & -\omega_\gamma & \omega_\psi\\ \omega_\gamma & 0 & -\omega_\phi\\ -\omega_\psi & \omega_\phi & 0\end{bmatrix}\boldsymbol{J}\boldsymbol{\omega}+\boldsymbol{u}+\boldsymbol{D} \tag{4}$$

where $\boldsymbol{J}=\mathrm{diag}(J_{\phi\phi}, J_{\psi\psi}, J_{\gamma\gamma})\in\mathbf{R}^{3\times3}$ is the inertia matrix of the launch vehicle; $\boldsymbol{u}\in\mathbf{R}^3$ the control torque vector; and $\boldsymbol{D}=[D_\phi \quad D_\psi \quad D_\gamma]^{\mathrm{T}}$ the unknown disturbance vector, including uncertain terms and external uncertainties caused by unmodeled dynamics of the system, changes in the moment of inertia due to fuel consumption of the launch vehicle and sloshing in the tanks, etc.

Let $\boldsymbol{x}_1=\boldsymbol{\Omega}$, $\boldsymbol{x}_2=\boldsymbol{Z}(\boldsymbol{\Omega})\boldsymbol{\omega}$, then the dynamics model of the launch vehicle can be represented as

$$\begin{cases}\dot{\boldsymbol{x}}_1=\boldsymbol{x}_2\\ \dot{\boldsymbol{x}}_2=\boldsymbol{f}_1(\boldsymbol{x}_1,\boldsymbol{x}_2)+\boldsymbol{f}_2(\boldsymbol{x}_1)\boldsymbol{u}+\boldsymbol{d}\end{cases} \tag{5}$$

where the specific forms of $\boldsymbol{f}_1(\boldsymbol{x}_1,\boldsymbol{x}_2)$, $\boldsymbol{f}_2(\boldsymbol{x}_1)$ and $\boldsymbol{d}$ are

$$\begin{cases}\boldsymbol{f}_1(\boldsymbol{x}_1,\boldsymbol{x}_2)=\dot{\boldsymbol{Z}}(\boldsymbol{x}_1)\boldsymbol{Z}^{-1}(\boldsymbol{x}_1)\boldsymbol{x}_2+\boldsymbol{Z}(\boldsymbol{x}_1)\\ \qquad \boldsymbol{F}(\boldsymbol{Z}^{-1}(\boldsymbol{x}_1)\boldsymbol{x}_2)\\ \boldsymbol{f}_2(\boldsymbol{x}_1)=\boldsymbol{Z}(\boldsymbol{x}_1)\boldsymbol{J}^{-1}\\ \boldsymbol{d}=\boldsymbol{Z}(\boldsymbol{x}_1)\boldsymbol{J}^{-1}\boldsymbol{D}\end{cases} \tag{6}$$

1.2 Launch vehicle attitude control system model with actuator faults

1.2.1 Launch vehicle actuator fault model

This article primarily considers the two most common types of actuator faults: Actuator efficiency loss fault and bias fault. The fault model of the actuator can be represented as[7]

$$\boldsymbol{\delta}_f=\boldsymbol{\rho}\boldsymbol{\delta}+\boldsymbol{\theta} \tag{7}$$

where $\boldsymbol{\rho}=\mathrm{diag}(\rho_1,\rho_2,\rho_3)\in\mathbf{R}^{3\times3}$ represents the efficiency coefficient matrix of the equivalent actuator, $\rho_i(i=1,2,3)$ is the efficiency coefficient when the actuator experiences efficiency loss, and $0<\rho_i<1$; $\boldsymbol{\theta}=[\theta_1 \quad \theta_2 \quad \theta_3]^{\mathrm{T}}$ the equivalent bias vector for bias-type faults, $\theta_i(i=1,2,3)$ is the bias amount of the three channels when the actuator experiences a bias-type fault. The fault model in Eq.(7) represents three scenarios: (1) No-fault condition: $\boldsymbol{\rho}=\boldsymbol{I}$ and $\boldsymbol{\theta}=\boldsymbol{0}$; (2) bias-type fault condition: $\boldsymbol{\rho}=\boldsymbol{I}$ and $\boldsymbol{\theta}\neq\boldsymbol{0}$; (3) efficiency loss fault condition: $\boldsymbol{0}<\boldsymbol{\rho}<\boldsymbol{I}$ and $\boldsymbol{\theta}=\boldsymbol{0}$.

1.2.2 Launch vehicle control system fault model

According to Eqs.(2,7), the fault model for system (5) is

$$\begin{cases}\dot{\boldsymbol{x}}_1=\boldsymbol{x}_2\\ \dot{\boldsymbol{x}}_2=\boldsymbol{f}_1(\boldsymbol{x}_1,\boldsymbol{x}_2)+\boldsymbol{f}_2(\boldsymbol{x}_1)\boldsymbol{B}\boldsymbol{\delta}_f+\boldsymbol{d}\end{cases} \tag{8}$$

where the specific forms of $\boldsymbol{f}_1(\boldsymbol{x}_1,\boldsymbol{x}_2)$, $\boldsymbol{f}_2(\boldsymbol{x}_1)$ and $\boldsymbol{d}$ are as shown in Eq.(6).

Remark 1 The fault issues considered in this paper are of the limited type. Due to the redundancy of the eight engines, after a fault occurs, the equivalent three-channel actuator still possesses a certain degree of control capability.

1.3 Launch vehicle attitude tracking system model with actuator faults

This paper studies the command tracking problem of the attitude control system of a launch vehicle with actuator bias and efficiency loss faults. The attitude angle tracking command is denoted as $\boldsymbol{x}_{1d}$, and the corresponding tracking error as $\boldsymbol{e}_1=\boldsymbol{x}_1-\boldsymbol{x}_{1d}$, that is $\boldsymbol{e}_2=\dot{\boldsymbol{e}}_1=\boldsymbol{x}_2-\dot{\boldsymbol{x}}_{1d}$. Therefore, the system (8) can be transformed into the command tracking error system

$$\begin{cases}\dot{\boldsymbol{e}}_1=\boldsymbol{e}_2\\ \dot{\boldsymbol{e}}_2=\ddot{\boldsymbol{e}}_1=\dot{\boldsymbol{x}}_2-\ddot{\boldsymbol{x}}_{1d}=\\ \qquad \boldsymbol{f}_1(\boldsymbol{x}_1,\boldsymbol{x}_2)+\boldsymbol{f}_2(\boldsymbol{x}_1)\boldsymbol{B}\boldsymbol{\delta}_f+\boldsymbol{d}-\ddot{\boldsymbol{x}}_{1d}\end{cases} \tag{9}$$

Remark 2 This paper takes the control system of a rocket with eight engines as an example to describe the modeling process of the launch vehicle control system, and ultimately derives the command tracking error system model. In reality, whether it has eight or six engines, the main difference is only in the specific transformation matrix involved in the control torque, and the rest are the same. Therefore, the command tracking error system described in this section is universal and applicable to the attitude fault-tolerant control problem of launch vehicles with different numbers of engines.

Throughout this paper, the following assumptions and lemma are introduced, which are needed in the sequel.

Assumption 1 The attitude angle command signal is continuous, and its first two derivatives are uniformly continuous and bounded[16].

Lemma 1[17-19] Define a function $F(\boldsymbol{\Lambda})$ in a compact set $\Omega_{\boldsymbol{\Lambda}}$, for any positive number ε, there exists a fuzzy logic system that satisfies

$$F(\boldsymbol{\Lambda})=\boldsymbol{W}^{\mathrm{T}}\boldsymbol{S}(\boldsymbol{\Lambda})+\xi(\boldsymbol{\Lambda}) \quad |\xi(\boldsymbol{\Lambda})|<\varepsilon \tag{10}$$

where $\xi(\boldsymbol{\Lambda})$ represents the approximation error; $\boldsymbol{W}=[\omega_1\ \omega_2\ \cdots\ \omega_m]^{\mathrm{T}}\in\mathbf{R}^m$ the desired weight vector; $\boldsymbol{S}(\boldsymbol{\Lambda})=\dfrac{[s_1(\boldsymbol{\Lambda})\ s_2(\boldsymbol{\Lambda})\ \cdots\ s_m(\boldsymbol{\Lambda})]^{\mathrm{T}}}{\sum_{j=1}^{m}s_j(\boldsymbol{\Lambda})}$ the fuzzy basis function vector ;$s_j(\boldsymbol{\Lambda})=\exp\left[\dfrac{-(\boldsymbol{\Lambda}-\boldsymbol{z}_j)^{\mathrm{T}}(\boldsymbol{\Lambda}-\boldsymbol{z}_j)}{\zeta_j^2}\right]$, $m>1$, $j=1,2,\cdots,m$; $\boldsymbol{z}_j=[z_{j1}\quad z_{j2}\quad\cdots\quad z_{jq}]^{\mathrm{T}}$ and ζ_j represent the center and the width of the basis functions, respectively.

Lemma 2 (Young's inequality) $a,b>0$, $\dfrac{1}{p}+\dfrac{1}{q}=1$, then

$$ab\leqslant\frac{a^p}{p}+\frac{b^q}{q} \tag{11}$$

where the equality holds if and only if $a^p=b^q$.

Lemma 3[20] Consider a nonlinear system $\dot{x}(t)=f(x(t))$, where $x(t)$ represents the system state and $f(\cdot)$ represents the nonlinear function. If there exists a positive definite continuous function $V(x(t))$, which satisfies

$$\dot{V}(x(t))\leqslant-mV^{\eta}(x(t)) \tag{12}$$

where $m>0$, $0<\eta<1$, then the system is said to be finite-time stable.

Lemma 4[21] Consider a nonlinear system $\dot{x}(t)=f(x(t))$, where $x(t)$ represents the system state and $f(\cdot)$ represents the nonlinear function. If there exists a positive definite continuous function $V(x(t))$, which satisfies

$$\dot{V}(x(t))\leqslant-mV^{\eta}(x(t))+v \tag{13}$$

where $m>0$, $v>0$, $0<\eta<1$, then the system is said to be semi-globally practically finite-time stable.

2 Main Results

The objective of attitude tracking control for a launch vehicle is to design a controller that ensures the attitude angle tracking error $\boldsymbol{e}_1$ can converges to zero within a finite time. For the system defined by Eq.(9), this paper proposes an adaptive super-twisting SMC law. By employing the super-twisting SMC method, system chattering is eliminated. Furthermore, to address system parameter variations, fuzzy logic control is utilized to approximate the unknown system terms. Adaptive control terms are introduced to compensate for disturbances and approximation errors, thereby enhancing closed-loop system stability and improving transient performance.

2.1 Design of adaptive super-twisting sliding mode fault-tolerant controller

The form of the super-twisting algorithm is as follows.

According to the instruction tracking error system of Eq.(9), the sliding mode surface is defined as

$$\boldsymbol{s}=\boldsymbol{c}\cdot\boldsymbol{e}_1+\boldsymbol{e}_2 \tag{14}$$

where $\boldsymbol{s}=[s_1\quad s_2\quad s_3]^{\mathrm{T}}\in\mathbf{R}^3$ and $\boldsymbol{c}=\mathrm{diag}(c_1,c_2,c_3)\in\mathbf{R}^{3\times3}$ are the parameters to be designed, satisfying $c_i>0, i=1,2,3$.

The sliding mode approach law is selected as

$$\dot{\boldsymbol{s}}=-\boldsymbol{\lambda}\cdot\boldsymbol{S}\cdot\mathrm{sign}(\boldsymbol{s})+\boldsymbol{\nu}\dot{\boldsymbol{\nu}}=-\boldsymbol{\alpha}\cdot\mathrm{sign}(\boldsymbol{s}) \tag{15}$$

where $\boldsymbol{\lambda}$ and $\boldsymbol{\alpha}$ are the parameters to be designed, $\boldsymbol{\lambda}=\mathrm{diag}(\lambda_1,\lambda_2,\lambda_3)\in\mathbf{R}^{3\times3}$, $\boldsymbol{\alpha}=\mathrm{diag}(\alpha_1,\alpha_2,\alpha_3)\in\mathbf{R}^{3\times3}$, with λ_i, $\alpha_i>0$, $\boldsymbol{S}=\mathrm{diag}\left(|s_1|^{\frac{1}{2}},|s_2|^{\frac{1}{2}},|s_3|^{\frac{1}{2}}\right)\in\mathbf{R}^{3\times3}$, $\boldsymbol{\nu}=[\nu_1\quad\nu_2\quad\nu_3]^{\mathrm{T}}\in\mathbf{R}^3$, $\mathrm{sign}(\boldsymbol{s})=[\mathrm{sign}(s_1),\mathrm{sign}(s_2),\mathrm{sign}(s_3)]^{\mathrm{T}}\in\mathbf{R}^3$.

Based on the above information, a fault-tolerant control scheme is proposed to ensure the asymptotic stability of system (9). The adaptive super-twisting sliding mode fault-tolerant control law is designed as follows.

For the attitude control system of the launch vehicle (9), if Assumption 1 holds, the adaptive super-twisting sliding mode controller designed according to Eq.(16) ensures that the system tracks the reference signal within a finite time, with the control law as

$$\begin{aligned}\boldsymbol{\delta}=&(f_2(\boldsymbol{x}_1)B)^{-1}(-\boldsymbol{\lambda}\cdot\boldsymbol{S}\cdot\mathrm{sign}(\boldsymbol{s}))+\\&(f_2(\boldsymbol{x}_1)B)^{-1}\left(\boldsymbol{\nu}-\boldsymbol{c}\cdot\boldsymbol{e}_2-\frac{1}{2}\hat{\boldsymbol{\Xi}}-\frac{1}{2}\boldsymbol{s}\right)+\\&(f_2(\boldsymbol{x}_1)B)^{-1}(-\boldsymbol{f}_1(\boldsymbol{x}_1,\boldsymbol{x}_2))+\\&(f_2(\boldsymbol{x}_1)B)^{-1}\left(-\boldsymbol{f}_2(\boldsymbol{x}_1)B\hat{\boldsymbol{\theta}}-\hat{\boldsymbol{d}}+\ddot{\boldsymbol{x}}_{1d}\right)\end{aligned}\tag{16}$$

where

$$\hat{\boldsymbol{\Xi}}=\begin{bmatrix}s_1\hat{P}_1\boldsymbol{S}_1^{\mathrm{T}}(\boldsymbol{\Lambda})\boldsymbol{S}_1(\boldsymbol{\Lambda})\\s_2\hat{P}_2\boldsymbol{S}_2^{\mathrm{T}}(\boldsymbol{\Lambda})\boldsymbol{S}_2(\boldsymbol{\Lambda})\\s_3\hat{P}_3\boldsymbol{S}_3^{\mathrm{T}}(\boldsymbol{\Lambda})\boldsymbol{S}_3(\boldsymbol{\Lambda})\end{bmatrix}\tag{17}$$

The adaptive laws is defined as

$$\dot{\hat{P}}_i=s_i^{\,2}\boldsymbol{S}_i^{\mathrm{T}}(\boldsymbol{\Lambda})\boldsymbol{S}_i(\boldsymbol{\Lambda})\quad i=1,2,3\tag{18}$$

$$\dot{\hat{\boldsymbol{\theta}}}=\boldsymbol{f}_2^{\mathrm{T}}(\boldsymbol{x}_1)\boldsymbol{s}\tag{19}$$

$$\dot{\hat{\boldsymbol{d}}}=\boldsymbol{s}\tag{20}$$

2.2 Stability analysis

In the previous section, a new fault-tolerant control scheme is developed. Then the stability of the fuzzy system (9) with the designed controllers (16—20) will be analyzed in this section.

Define $\boldsymbol{x}_1=[\phi\ \ \psi\ \ \gamma]^{\mathrm{T}}\in\mathbf{R}^3$, $\boldsymbol{e}_1=[e_{11}\ \ e_{12}\ \ e_{13}]^{\mathrm{T}}$, $\hat{\boldsymbol{\theta}}=\left[\hat{\theta}_1\ \ \hat{\theta}_2\ \ \hat{\theta}_3\right]^{\mathrm{T}}$ and $\hat{\boldsymbol{d}}=\left[\hat{d}_1\ \ \hat{d}_2\ \ \hat{d}_3\right]^{\mathrm{T}}$. The following theorem provides the asymptotic stability analysis for the system (9) with the proposed controller and the adaptive laws in Eqs.(16—20).

Theorem 1 Consider the closed-loop system (9). Suppose that Assumption 1 and inequalities in Eqs. (10—13), command tracking error $\boldsymbol{e}_1(t)$, $\hat{\boldsymbol{\theta}}$, and $\hat{\boldsymbol{d}}$ of the system are uniformly bounded. Moreover, $\boldsymbol{e}_1(t)$ converges to zero asymptotically within a finite time.

Proof

Step 1 For the sliding mode approach rate shown in Eq. (15), the following Lyapunov function is defined

$$V_1=\frac{1}{2}\boldsymbol{s}^{\mathrm{T}}\boldsymbol{s}\tag{21}$$

It can be seen from Eq.(21), $V_1>0$ and by taking the derivative, we can get

$$\begin{aligned}V_1=&\boldsymbol{s}^{\mathrm{T}}\dot{\boldsymbol{s}}=\\&s_1\left(-\lambda_1|s_1|^{\frac{1}{2}}\mathrm{sign}(s_1)-\int\alpha_1\cdot\mathrm{sign}(s_1)\mathrm{d}t\right)+\\&s_2\left(-\lambda_2|s_2|^{\frac{1}{2}}\mathrm{sign}(s_2)-\int\alpha_2\cdot\mathrm{sign}(s_2)\mathrm{d}t\right)+\\&s_3\left(-\lambda_3|s_3|^{\frac{1}{2}}\mathrm{sign}(s_3)-\int\alpha_3\cdot\mathrm{sign}(s_3)\mathrm{d}t\right)=\\&-\vartheta_1|s_1|-\vartheta_2|s_2|-\vartheta_3|s_3|\leqslant\\&-\vartheta_1s_1-\vartheta_2s_2-\vartheta_3s_3\leqslant\\&-\vartheta\cdot\left(\left(\frac{1}{2}s_1^2\right)^{\frac{1}{2}}+\left(\frac{1}{2}s_2^2\right)^{\frac{1}{2}}+\left(\frac{1}{2}s_3^2\right)^{\frac{1}{2}}\right)\leqslant\\&-\vartheta\cdot\left(\left(\frac{1}{2}s_1^2+\frac{1}{2}s_2^2+\frac{1}{2}s_3^2\right)^{\frac{1}{2}}\right)\leqslant-\vartheta V_1^{\frac{1}{2}}\end{aligned}\tag{22}$$

where $\lambda_i>0$, $\alpha_i>0$, so $\vartheta_i=\lambda_i|s_i|^{\frac{1}{2}}+\int\alpha_i\mathrm{d}t>0$, $\vartheta=\min\{\vartheta_1,\vartheta_2,\vartheta_3\}>0$. Moreover, in the design of the control law, $\dot{V}\leqslant-\vartheta V_1^{\frac{1}{2}}$, according to Lemma 3, we can ensure that the attitude tracking error converges to zero in a finite time along the super-twisting sliding mode surface.

Step 2 For system (9), the Lyapunov function is defined as

$$V=\frac{1}{2}\boldsymbol{s}^{\mathrm{T}}\boldsymbol{s}+\frac{1}{2}\tilde{\boldsymbol{\theta}}^{\mathrm{T}}\tilde{\boldsymbol{\theta}}+\frac{1}{2}\tilde{\boldsymbol{d}}^{\mathrm{T}}\tilde{\boldsymbol{d}}+\frac{1}{4}\tilde{P}_1^2+\frac{1}{4}\tilde{P}_2^2+\frac{1}{4}\tilde{P}_3^2\tag{23}$$

where $\tilde{\boldsymbol{\theta}}=\boldsymbol{\theta}-\hat{\boldsymbol{\theta}}$, $\tilde{\boldsymbol{d}}=\boldsymbol{d}-\hat{\boldsymbol{d}}$ and $\tilde{P}_i=P_i-\hat{P}_i$, "$\tilde{\cdot}$" represents the error between the measured value and the observed value; "$\cdot$" the measured value; "$\hat{\cdot}$" the observer.

Then the derivative of V satisfies

$$\dot{V}=\boldsymbol{s}^{\mathrm{T}}\dot{\boldsymbol{s}}-\tilde{\boldsymbol{\theta}}^{\mathrm{T}}\dot{\hat{\boldsymbol{\theta}}}-\tilde{\boldsymbol{d}}^{\mathrm{T}}\dot{\hat{\boldsymbol{d}}}-\frac{1}{2}\tilde{P}_1\dot{\hat{P}}_1-\frac{1}{2}\tilde{P}_2\dot{\hat{P}}_2-\frac{1}{2}\tilde{P}_3\dot{\hat{P}}_3\tag{24}$$

The derivative of the sliding mode surface $\boldsymbol{s}$ in Eq.(14) takes the derivative of t to get

$$\boldsymbol{s}=\boldsymbol{c}\cdot\dot{\boldsymbol{e}}_1+\dot{\boldsymbol{e}}_2=\boldsymbol{c}\cdot\boldsymbol{e}_2+\boldsymbol{f}_1(\boldsymbol{x}_1,\boldsymbol{x}_2)+\boldsymbol{f}_2(\boldsymbol{x}_1)\boldsymbol{u}_f+\boldsymbol{d}-\ddot{\boldsymbol{x}}_{1d}\tag{25}$$

By inserting Eqs.(6, 7) into Eq.(25), we get

$$\begin{aligned}\dot{\boldsymbol{s}}=&\boldsymbol{c}\cdot\boldsymbol{e}_2+\boldsymbol{f}_1(\boldsymbol{x}_1,\boldsymbol{x}_2)+\boldsymbol{f}_2(\boldsymbol{x}_1)\boldsymbol{u}_f+\boldsymbol{d}-\ddot{\boldsymbol{x}}_{1d}=\\&\boldsymbol{c}\cdot\boldsymbol{e}_2+\boldsymbol{f}_1(\boldsymbol{x}_1,\boldsymbol{x}_2)+\boldsymbol{f}_2(\boldsymbol{x}_1)B(\boldsymbol{\rho}\boldsymbol{\delta}+\boldsymbol{\theta})+\boldsymbol{d}-\ddot{\boldsymbol{x}}_{1d}=\\&\boldsymbol{c}\cdot\boldsymbol{e}_2+\boldsymbol{f}_1(\boldsymbol{x}_1,\boldsymbol{x}_2)+\boldsymbol{f}_2(\boldsymbol{x}_1)B\boldsymbol{\delta}+\\&\boldsymbol{f}_2(\boldsymbol{x}_1)B(\boldsymbol{\rho}-\boldsymbol{I})\boldsymbol{\delta}+\boldsymbol{f}_2(\boldsymbol{x}_1)B\boldsymbol{\theta}+\boldsymbol{d}-\ddot{\boldsymbol{x}}_{1d}=\\&\boldsymbol{c}\cdot\boldsymbol{e}_2+\boldsymbol{f}_1(\boldsymbol{x}_1,\boldsymbol{x}_2)+\boldsymbol{f}_2(\boldsymbol{x}_1)B\boldsymbol{\delta}+F(\boldsymbol{\Lambda})+\\&\boldsymbol{f}_2(\boldsymbol{x}_1)B\boldsymbol{\theta}+\boldsymbol{d}-\ddot{\boldsymbol{x}}_{1d}\end{aligned}\tag{26}$$

where

$$F(\boldsymbol{\Lambda})=[F_1(\boldsymbol{\Lambda}_1)\quad F_2(\boldsymbol{\Lambda}_2)\quad F_3(\boldsymbol{\Lambda}_3)]^{\mathrm{T}}= \boldsymbol{f}_2(\boldsymbol{x}_1)B(\boldsymbol{\rho}-\boldsymbol{I})\boldsymbol{\delta} \tag{27}$$

where

$$\boldsymbol{\Lambda}=[\boldsymbol{\Lambda}_1\quad \boldsymbol{\Lambda}_2\quad \boldsymbol{\Lambda}_3]= [\boldsymbol{x}_1^{\mathrm{T}},\ \boldsymbol{x}_2^{\mathrm{T}},\ \dot{\boldsymbol{x}}_2^{\mathrm{T}},\ \boldsymbol{x}_{1d}^{\mathrm{T}},\ \dot{\boldsymbol{x}}_{1d}^{\mathrm{T}},\ \ddot{\boldsymbol{x}}_{1d}^{\mathrm{T}}]^{\mathrm{T}}$$

In Eq. (27), $F_i(\boldsymbol{\Lambda}_i)$ is an unknown nonlinear function, which this paper approximates using the fuzzy logic control as

$$F(\boldsymbol{\Lambda})=[F_1(\boldsymbol{\Lambda}_1)\quad F_2(\boldsymbol{\Lambda}_2)\quad F_3(\boldsymbol{\Lambda}_3)]^{\mathrm{T}}= \begin{bmatrix} \boldsymbol{W}_1^{\mathrm{T}}\boldsymbol{S}_1(\boldsymbol{\Lambda}_1)+s_1\sigma_1(\boldsymbol{\Lambda}_1) \\ \boldsymbol{W}_2^{\mathrm{T}}\boldsymbol{S}_2(\boldsymbol{\Lambda}_1)+s_2\sigma_2(\boldsymbol{\Lambda}_1) \\ \boldsymbol{W}_3^{\mathrm{T}}\boldsymbol{S}_3(\boldsymbol{\Lambda}_1)+s_3\sigma_3(\boldsymbol{\Lambda}_1) \end{bmatrix} \tag{28}$$

Substituting Eq. (26) into Eq. (24) yields

$$\begin{aligned} V={}&\boldsymbol{s}^{\mathrm{T}}\dot{\boldsymbol{s}}-\tilde{\theta}^{\mathrm{T}}\dot{\hat{\theta}}-\tilde{\boldsymbol{d}}^{\mathrm{T}}\dot{\hat{\boldsymbol{d}}}-\frac{1}{2}\tilde{P}_1\dot{\hat{P}}_1-\frac{1}{2}\tilde{P}_2\dot{\hat{P}}_2-\frac{1}{2}\tilde{P}_3\dot{\hat{P}}_3= \\ &\boldsymbol{s}^{\mathrm{T}}(\boldsymbol{c}\bullet\boldsymbol{e}_2+\boldsymbol{f}_1(\boldsymbol{x}_1,\boldsymbol{x}_2)+\boldsymbol{f}_2(\boldsymbol{x}_1)B\boldsymbol{\delta})+ \\ &\boldsymbol{s}^{\mathrm{T}}(F(\boldsymbol{\Lambda})+\boldsymbol{f}_2(\boldsymbol{x}_1)B\boldsymbol{\theta}+\boldsymbol{d}-\ddot{x}_{1d})-\tilde{\boldsymbol{\theta}}^{\mathrm{T}}\dot{\hat{\boldsymbol{\theta}}}- \\ &\tilde{\boldsymbol{d}}^{\mathrm{T}}\dot{\hat{\boldsymbol{d}}}-\frac{1}{2}\tilde{P}_1\dot{\hat{P}}_1-\frac{1}{2}\tilde{P}_2\dot{\hat{P}}_2-\frac{1}{2}\tilde{P}_3\dot{\hat{P}}_3 \end{aligned} \tag{29}$$

By substituting Eqs. (16—20), we get

$$\begin{aligned} \dot{V}={}&\boldsymbol{s}^{\mathrm{T}}\left(-\boldsymbol{\lambda}\bullet\boldsymbol{S}\bullet\mathrm{sign}(\boldsymbol{s})+\boldsymbol{v}-\frac{1}{2}\hat{\boldsymbol{\Xi}}\right)+ \\ &\boldsymbol{s}^{\mathrm{T}}\left(-\boldsymbol{f}_2(\boldsymbol{x}_1)B\hat{\boldsymbol{\theta}}-\hat{\boldsymbol{d}}-\frac{1}{2}\boldsymbol{s}\right)+ \\ &\boldsymbol{s}^{\mathrm{T}}F(\boldsymbol{\Lambda})+\boldsymbol{s}^{\mathrm{T}}\boldsymbol{f}_2(\boldsymbol{x}_1)B\boldsymbol{\theta}+\boldsymbol{s}^{\mathrm{T}}\boldsymbol{d}- \\ &\tilde{\boldsymbol{\theta}}^{\mathrm{T}}\dot{\hat{\boldsymbol{\theta}}}-\tilde{\boldsymbol{d}}^{\mathrm{T}}\dot{\hat{\boldsymbol{d}}}-\frac{1}{2}\tilde{P}_1\dot{\hat{P}}_1-\frac{1}{2}\tilde{P}_2\dot{\hat{P}}_2-\frac{1}{2}\tilde{P}_3\dot{\hat{P}}_3= \\ &\boldsymbol{s}^{\mathrm{T}}(-\boldsymbol{\lambda}\bullet\boldsymbol{S}\bullet\mathrm{sign}(\boldsymbol{s})+\boldsymbol{\nu})-\frac{1}{2}\boldsymbol{s}^{\mathrm{T}}\hat{\boldsymbol{\Xi}}- \\ &\boldsymbol{s}^{\mathrm{T}}\boldsymbol{f}_2(\boldsymbol{x}_1)B\hat{\boldsymbol{\theta}}-\boldsymbol{s}^{\mathrm{T}}\hat{\boldsymbol{d}}-\frac{1}{2}\boldsymbol{s}^{\mathrm{T}}\boldsymbol{s}+ \\ &\boldsymbol{s}^{\mathrm{T}}F(\boldsymbol{\Lambda})+\boldsymbol{s}^{\mathrm{T}}\boldsymbol{f}_2(\boldsymbol{x}_1)B\boldsymbol{\theta}+\boldsymbol{s}^{\mathrm{T}}\boldsymbol{d}- \\ &\tilde{\boldsymbol{\theta}}^{\mathrm{T}}B^{\mathrm{T}}\boldsymbol{f}_2^{\mathrm{T}}(\boldsymbol{x}_1)\boldsymbol{s}-\tilde{\boldsymbol{d}}^{\mathrm{T}}\boldsymbol{s}- \\ &\frac{1}{2}\tilde{P}_1s_1^2\boldsymbol{S}_1^{\mathrm{T}}(\boldsymbol{\Lambda})\boldsymbol{S}_1(\boldsymbol{\Lambda})-\frac{1}{2}\tilde{P}_2s_2^2\boldsymbol{S}_2^{\mathrm{T}}(\boldsymbol{\Lambda})\boldsymbol{S}_2(\boldsymbol{\Lambda})- \\ &\frac{1}{2}\tilde{P}_3s_3^2\boldsymbol{S}_3^{\mathrm{T}}(\boldsymbol{\Lambda})\boldsymbol{S}_3(\boldsymbol{\Lambda}) \end{aligned} \tag{30}$$

According to Lemma 2 (Young's inequality), we have

$$\begin{aligned} \boldsymbol{s}^{\mathrm{T}}F(\boldsymbol{\Lambda})={}&\boldsymbol{s}^{\mathrm{T}}[F_1(\boldsymbol{\Lambda}_1)\quad F_2(\boldsymbol{\Lambda}_2)\quad F_3(\boldsymbol{\Lambda}_3)]^{\mathrm{T}}= \\ &s_1\boldsymbol{W}_1^{\mathrm{T}}\boldsymbol{S}_1(\boldsymbol{\Lambda}_1)+s_1\sigma_1(\boldsymbol{\Lambda}_1)+s_2\boldsymbol{W}_2^{\mathrm{T}}\boldsymbol{S}_2(\boldsymbol{\Lambda}_2)+ \\ &s_2\sigma_2(\boldsymbol{\Lambda}_2)+s_3\boldsymbol{W}_3^{\mathrm{T}}\boldsymbol{S}_3(\boldsymbol{\Lambda}_3)+s_3\sigma_3(\boldsymbol{\Lambda}_3)\leqslant \\ &\frac{s_1^2P_1\boldsymbol{S}_1^{\mathrm{T}}(\boldsymbol{\Lambda}_1)\boldsymbol{S}_1(\boldsymbol{\Lambda}_1)}{2}+\frac{s_1^2}{2}+\frac{\sigma_1^2}{2}+ \\ &\frac{s_2^2P_2\boldsymbol{S}_2^{\mathrm{T}}(\boldsymbol{\Lambda}_2)\boldsymbol{S}_2(\boldsymbol{\Lambda}_2)}{2}+\frac{s_2^2}{2}+\frac{\sigma_2^2}{2}+ \\ &\frac{s_3^2P_3\boldsymbol{S}_3^{\mathrm{T}}(\boldsymbol{\Lambda}_3)\boldsymbol{S}_3(\boldsymbol{\Lambda}_3)}{2}+\frac{s_3^2}{2}+\frac{\sigma_3^2}{2}\leqslant \\ &\frac{s_1^2P_1\boldsymbol{S}_1^{\mathrm{T}}(\boldsymbol{\Lambda}_1)\boldsymbol{S}_1(\boldsymbol{\Lambda}_1)}{2}+\frac{s_2^2P_2\boldsymbol{S}_2^{\mathrm{T}}(\boldsymbol{\Lambda}_2)\boldsymbol{S}_2(\boldsymbol{\Lambda}_2)}{2}+ \\ &\frac{s_3^2P_3\boldsymbol{S}_3^{\mathrm{T}}(\boldsymbol{\Lambda}_3)\boldsymbol{S}_3(\boldsymbol{\Lambda}_3)}{2}+\frac{\boldsymbol{s}^{\mathrm{T}}\boldsymbol{s}}{2}+\frac{\varepsilon_1^2+\varepsilon_2^2+\varepsilon_3^2}{2} \end{aligned} \tag{31}$$

where in an unknown variable $P_i=\|\boldsymbol{W}_i\|$ is defined.

Substituting Eq. (31) into Eq. (30), we get

$$\begin{aligned} \dot{V}\leqslant{}&\boldsymbol{s}^{\mathrm{T}}(-\boldsymbol{\lambda}\bullet\boldsymbol{S}\bullet\mathrm{sign}(\boldsymbol{s})+\boldsymbol{v})-\frac{1}{2}\boldsymbol{s}^{\mathrm{T}}\hat{\boldsymbol{\Xi}}- \\ &\boldsymbol{s}^{\mathrm{T}}\boldsymbol{f}_2(\boldsymbol{x}_1)B\hat{\boldsymbol{\theta}}-\boldsymbol{s}^{\mathrm{T}}\hat{\boldsymbol{d}}-\frac{1}{2}\boldsymbol{s}^{\mathrm{T}}\boldsymbol{s}+ \\ &\frac{1}{2}s_1^2P_1\boldsymbol{S}_1^{\mathrm{T}}(\boldsymbol{\Lambda}_1)\boldsymbol{S}_1(\boldsymbol{\Lambda}_1)+\frac{1}{2}s_2^2P_2\boldsymbol{S}_2^{\mathrm{T}}(\boldsymbol{\Lambda}_2)\boldsymbol{S}_2(\boldsymbol{\Lambda}_2)+ \\ &\frac{1}{2}s_3^2P_3\boldsymbol{S}_3^{\mathrm{T}}(\boldsymbol{\Lambda}_3)\boldsymbol{S}_3(\boldsymbol{\Lambda}_3)+\frac{\boldsymbol{s}^{\mathrm{T}}\boldsymbol{s}}{2}+\frac{\varepsilon_1^2+\varepsilon_2^2+\varepsilon_3^2}{2}+ \\ &\boldsymbol{s}^{\mathrm{T}}\boldsymbol{f}_2(\boldsymbol{x}_1)B\boldsymbol{\theta}+\boldsymbol{s}^{\mathrm{T}}\boldsymbol{d}-\tilde{\boldsymbol{\theta}}^{\mathrm{T}}B^{\mathrm{T}}\boldsymbol{f}_2^{\mathrm{T}}(\boldsymbol{x}_1)\boldsymbol{s}-\tilde{\boldsymbol{d}}^{\mathrm{T}}\boldsymbol{s}- \\ &\frac{1}{2}\tilde{P}_1s_1^2\boldsymbol{S}_1^{\mathrm{T}}(\boldsymbol{\Lambda}_1)\boldsymbol{S}_1(\boldsymbol{\Lambda}_1)-\frac{1}{2}\tilde{P}_2s_2^2\boldsymbol{S}_2^{\mathrm{T}}(\boldsymbol{\Lambda}_2)\boldsymbol{S}_2(\boldsymbol{\Lambda}_2)- \\ &\frac{1}{2}\tilde{P}_3s_3^2\boldsymbol{S}_3^{\mathrm{T}}(\boldsymbol{\Lambda}_3)\boldsymbol{S}_3(\boldsymbol{\Lambda}_3)= \\ &\boldsymbol{s}^{\mathrm{T}}(-\boldsymbol{\lambda}\bullet\boldsymbol{S}\bullet\mathrm{sign}(\boldsymbol{s})+\boldsymbol{v})+\frac{\varepsilon_1^2+\varepsilon_2^2+\varepsilon_3^2}{2} \end{aligned} \tag{32}$$

where $\frac{\varepsilon_1^2+\varepsilon_2^2+\varepsilon_3^2}{2}$ is a positive real number, denoted as ς.

Combining Eq. (22), Eq. (33) is

$$\begin{aligned} \dot{V}\leqslant{}&\boldsymbol{s}^{\mathrm{T}}(-\boldsymbol{\lambda}\bullet\boldsymbol{S}\bullet\mathrm{sign}(\boldsymbol{s})+\boldsymbol{\nu})+\zeta\leqslant \\ &-\vartheta\bullet\left(\left(\frac{1}{2}s_1^2+\frac{1}{2}s_2^2+\frac{1}{2}s_3^2\right)^{\frac{1}{2}}\right)+\zeta\leqslant \\ &-\vartheta V^{\frac{1}{2}}+\tilde{\omega} \end{aligned} \tag{33}$$

where $\lambda_i>0$, $\alpha_i>0$, so $\vartheta_i=\lambda_i|s_i|^{\frac{1}{2}}+\int\alpha_i\mathrm{d}t>0$, $\vartheta=\min\{\vartheta_1,\vartheta_2,\vartheta_3\}>0$, and there must exist a real number $\tilde{\omega}$, makes $\tilde{\omega}\geqslant \vartheta\left(V^{\frac{1}{2}}-\left(\left(\frac{1}{2}s_1^2\right)^{\frac{1}{2}}+\left(\frac{1}{2}s_2^2\right)^{\frac{1}{2}}+\left(\frac{1}{2}s_3^2\right)^{\frac{1}{2}}\right)\right)+\varsigma$.

That is, in the control law design, $\dot{V}\leqslant-\vartheta V^{\frac{1}{2}}+\tilde{\omega}$, and according to Lemma 4, it can be guaranteed that the system is semi-globally practically finite-time stable. Therefore, the sliding surface is reachable in a finite time, and due to the super-twisting sliding mode characteristics, the attitude tracking error converges to zero in a finite time.

Theorem 2 The system (9) is semi-globally practically finite-time stable at the origin, with the tracking error converging to a small neighborhood around the origin in a finite time, and the upper bound of the convergence time t_s is

$$t_s=\frac{2}{\kappa_0\vartheta}\left[V^{\frac{1}{2}}(t=0)-\frac{\tilde{\omega}}{(1-\kappa_0)\vartheta}\right] \tag{34}$$

where $0<\kappa_0\leqslant 1$.

Remark 3 The conclusion of Theorem 2 is mainly based on Lemma 4 in Ref.[15]. The specific proof process can be found in Ref.[15], and will not be elaborated here.

3 Simulation Examples

This section presents simulation experiments to verify the effectiveness of the proposed adaptive super-twisting sliding mode fault-tolerant controller for the launch vehicle. The experiments demonstrate the controller's performance in the presence of actuator faults and unknown disturbances.

In the simulation example, the total simulation time is 60 s and the step length is 0.001 s. The specific parameter settings of the launch vehicle are shown in Table 1[22]. The initial value of the attitude angle and the initial value of the attitude angular velocity of the attitude control system of the launch vehicle are set as $\boldsymbol{\Omega}=[\phi \quad \psi \quad \gamma]^{\mathrm{T}}=[0^\circ \quad 0^\circ \quad 90^\circ]^{\mathrm{T}}$ and $\omega_\phi=\omega_\psi=\omega_\gamma=0/((^\circ)\cdot s^{-1})$. The attitude tracking command signal is set as $\boldsymbol{x}_{1d}=\boldsymbol{\Omega}_{1d}=[-10^\circ \quad 10^\circ \quad 70^\circ]^{\mathrm{T}}$, and the filter $G(s)=\dfrac{0.04}{s^2+0.4s+0.04}$ is used to smooth it, and the initial value of the attitude tracking command signal is the same as the initial value of the attitude angle of the attitude control system of the launch vehicle.

During the flight of a launch vehicle, the perturbations caused by unmodeled dynamic system behaviors, changes in rotational inertia due to fuel tank sloshing and consumption, and other factors are not necessarily constant disturbances. These unknown disturbances may have fluctuations at any time. Therefore, in simulations, considering the impact of various unknown disturbances on the launch vehicle's attitude control system, and based on the common disturbance models of launch vehicles in Ref.[21], the expression for external disturbances such as aerodynamic effects is set as $\boldsymbol{D}=0.05[\sin t \quad \cos(2t) \quad \sin(3t)]^{\mathrm{T}}$. The controller parameters are set as $\boldsymbol{c}_1=\mathrm{diag}(1, 1, 1)\in\mathbf{R}^{3\times 3}$, $\boldsymbol{\lambda}=\mathrm{diag}(88, 88, 88)\in\mathbf{R}^{3\times 3}$, $\boldsymbol{\alpha}=\mathrm{diag}(5, 5, 5)\in\mathbf{R}^{3\times 3}$.

Table 1 Parameters of the launch vehicle[22]

Parameter	Value
r/m	3.47
R/m	6.025
T/N	1 200 000
I_{xx}/(kg · m^2)	2 900 000
I_{yy},I_{zz}/(kg · m^2)	59 000 000
X_R/m	56.74
X_Z/m	66.667 8

To verify the effectiveness of the proposed adaptive super-twisting sliding mode fault-tolerant controller under different actuator fault situations and types, two distinct fault conditions are considered.

3.1 Multiple engine actuator faults situation

During a launch vehicle mission, in addition to the possibility of a single engine actuator fault, multiple engine failures may occur simultaneously. For potential multiple engine actuator faults, the following fault scenario is considered. The system operates fault-free before 20 s. After 20 s, booster engine 4 and core engine 1 experience bias faults of -3° and -1°, respectively. After 40 s, booster engine 2 experiences an efficiency loss fault of 50%. The simulation results are shown in Fig.2. Figs.2(a—c) depict the tracking trajectories of the roll, the yaw, and the pitch angles, respectively. Fig.2(d) shows the attitude angle tracking error curve, and Fig.2(e) displays the angular velocity variation curves.

Regarding the aforementioned fault, analysis of the engine layout indicates that the engine actuator fault at $t=20$ s and $t=40$ s affects the three axes of the launch vehicle to varying degrees. Simulation results show that all three axes exhibit tracking errors with amplitudes below 0.004 at the time of each fault. Compared with results in Refs.[7,15], the fault's impact is less significant, and the pro-

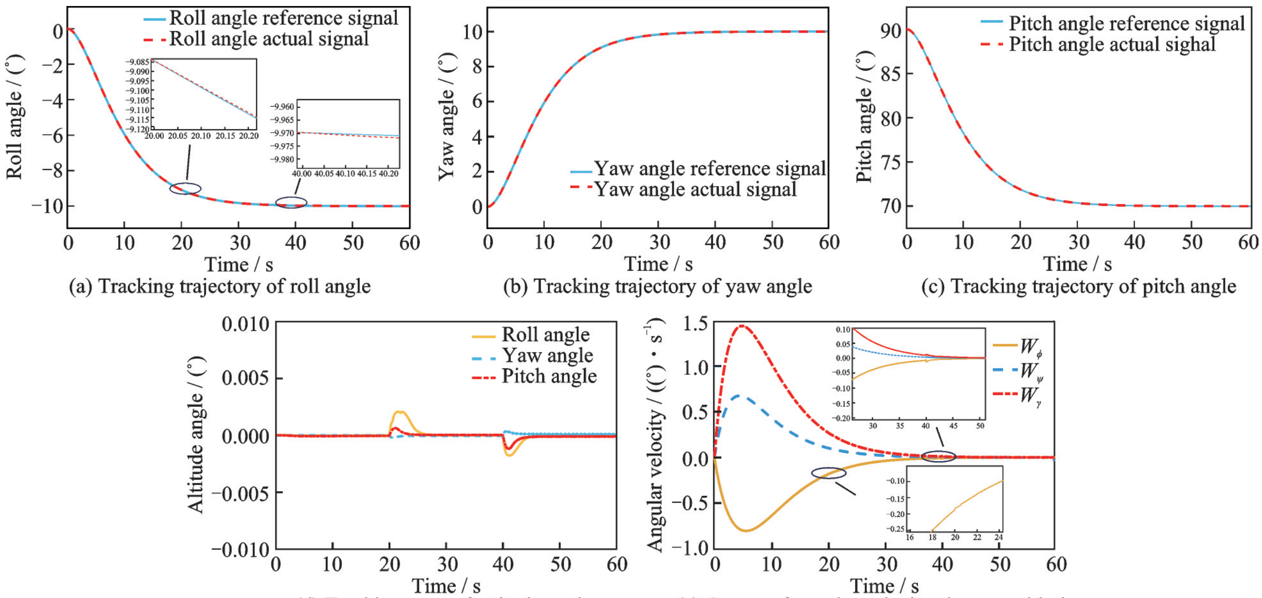

(a) Tracking trajectory of roll angle (b) Tracking trajectory of yaw angle (c) Tracking trajectory of pitch angle

(d) Tracking error of attitude angle (e) Curves of angular velocity changes with time

Fig.2 Multi-engine actuator faults

posed adaptive super-twisting sliding mode fault-tolerant controller demonstrates superior control accuracy and robustness.

3.2 Engine actuator time-varying fault situation

For the engine actuator, given possible time-varying faults due to external disturbances and mechanism aging, we consider the following actuator fault scenario. The system operates fault-free before 20 s. After 20 s, booster engine 3 experiences a time-varying bias fault, with a bias of $3+0.5\sin(0.5t)$. The simulation results are shown in Fig.3. Figs.3(a—c) depict the tracking trajectories of the roll, the yaw, and the pitch angles, respectively. Fig.3(d) shows the attitude angle tracking error curve, and Fig.3(e) displays the angular velocity variation curves.

Based on the identified fault and engine layout analysis, the failure of booster engine 3 primarily impacts the roll and the pitch axes. Simulation results show that both the roll and the yaw channels exhibit tracking errors with amplitudes less than 0.003 upon fault occurrence. Compared with results in Refs.[7, 15], the fault's impact is less signifi-

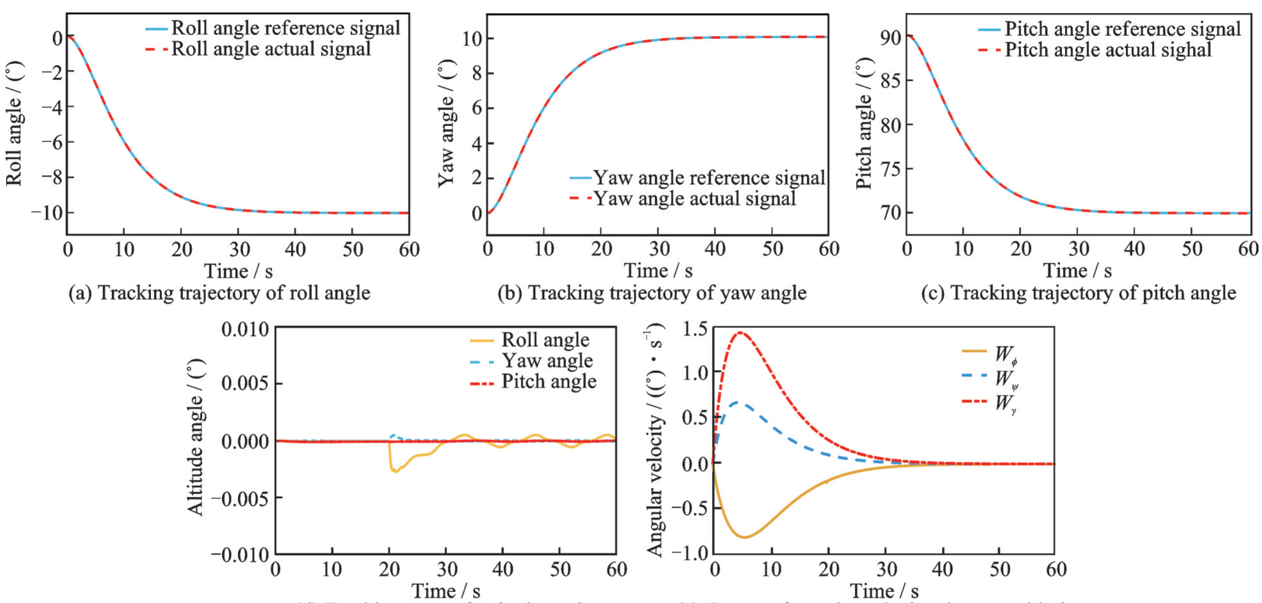

(a) Tracking trajectory of roll angle (b) Tracking trajectory of yaw angle (c) Tracking trajectory of pitch angle

(d) Tracking error of attitude angle (e) Curves of angular velocity changes with time

Fig.3 Time-varying actuator faults

cant, and the proposed adaptive super-twisting sliding mode fault-tolerant controller demonstrates superior control accuracy and robustness.

4 Conclusions

This paper proposes an adaptive super-twisting sliding mode fault-tolerant controller for the attitude control system of a launch vehicle, addressing uncertainties arising from unmodeled system dynamics, perturbations in rotational inertia due to fuel consumption and tank sloshing, actuator faults, and external disturbances. The designed controller ensures finite-time convergence to zero. Furthermore, it mitigates system chattering using the super-twisting SMC. In the presence of system parameter variations, a fuzzy logic system approximates unknown system terms, and adaptive control terms compensate for disturbances and approximation errors, ensuring good robustness. Simulation results validate the effectiveness, robustness, and good command tracking performance of the proposed controller. However, the method has limitations. This paper considered only certain types of uncertainties, and its robustness could be further improved for more complex nonlinear uncertainties and time-varying disturbances. Furthermore, the control method can be combined with advanced techniques such as model predictive control to further enhance the system performance and robustness. Moreover, the simulations are based on ideal actuator models. Future work should involve validation in more realistic hardware-in-the-loop simulations or even flight tests.

References

[1] LI Dong, YANG Yunfei, HU Pengxiang, et al. Research on multibody dynamic modeling and simulation technology for launch vehicles[J]. Journal of Astronautics, 2021, 42(2): 141-149. (in Chinese)

[2] LI D, LI P Q, WANG J, et al. General scheme and key technology of long March 5 launch vehicle[J]. Journal of Deep Space Exploration, 2021, 8(4): 335-343.

[3] QIAN Moshu, XIONG Ke, WANG Haiyang. Sliding mode dynamic surface control in precise recovery phase for reusable launch vehicle[J]. Journal of Astronautics, 2018, 39(8): 879-888. (in Chinese)

[4] XIE C, YANG S, CHENG Y, et al. Multiple model fault diagnosis and fault tolerant control for the launch vehicle's attitude control system[J]. The Aeronautical Journal, 2024, 128(1326): 1875-1894.

[5] ZHENG Y J, ZHENG J C, SHAO K, et al. Adaptive fuzzy sliding mode control of uncertain nonholonomic wheeled mobile robot with external disturbance and actuator saturation[J]. Information Sciences, 2024, 663: 120303.

[6] SONG X J, FAN Z W, LU S F, et al. Predefined-time sliding mode attitude control for liquid-filled spacecraft with large amplitude sloshing[J]. European Journal of Control, 2024, 77: 100970.

[7] WANG Peisheng, QU Dongyang, RAN Maopeng, et al. Adaptive sliding-mode control of launch vehicle with actuator failures[J]. Journal of Astronautics, 2023, 44(8): 1160-1170. (in Chinese)

[8] LIU Shijie, HUANG Zhilai, YANG Mingxing, et al. Fractional-order sliding mode control of robotic arms with boundary layer[J]. Journal of Shanghai University of Engineering Science, 2021, 35(4): 327-332. (in Chinese)

[9] ZHAO Xinyu, WANG Limei. Fractional order variable-gain super-twisting terminal sliding mode position control[EB/OL]. (2024-09-04). http://kns.cnki.net/kcms/detail/44.1240. TP. 20240830.1259.016. html. (in Chinese)

[10] LEVANT A. Sliding order and sliding accuracy in sliding mode control[J]. International Journal of Control, 1993, 58: 1247-1263.

[11] HU J B, ZHANG X, ZHANG D, et al. Finite-time adaptive super-twisting sliding mode control for autonomous robotic manipulators with actuator faults[J]. ISA Transactions, 2024, 144: 342-351.

[12] EL-SOUSY F F M, ALATTAS K A, MOFID O, et al. Robust adaptive super-twisting sliding mode stability control of underactuated rotational inverted pendulum with experimental validation[J]. IEEE Access, 2022, 10: 100857-100866.

[13] GONZALEZ-GARCIA A, CASTAÑEDA H, DE LEÓN-MORALES J. Unmanned surface vehicle robust tracking control using an adaptive super-twisting controller[J]. Control Engineering Practice, 2024, 149: 105985.

[14] HOU Q K, DING S H, YU X H. Composite super-twisting sliding mode control design for PMSM speed regulation problem based on a novel disturbance observer[J]. IEEE Transactions on Energy Conversion, 2021, 36(4): 2591-2599.

[15] MA Yanru, WANG Qing, HU Changhua, et al. Non-singular terminal sliding mode fault-tolerant control of launch vehicle with actuator fault[J]. Journal of Astronautics, 2020, 41(12): 1553-1560. (in Chinese)

[16] SHAO X D, HU Q L, SHI Y, et al. Fault-tolerant control for full-state error constrained attitude tracking of uncertain spacecraft[J]. Automatica, 2023, 151: 110907.

[17] WANG H Q, LIU P X, ZHAO X D, et al. Adaptive fuzzy finite-time control of nonlinear systems with actuator faults[J]. IEEE Transactions on Cybernetics, 2020, 50(5): 1786-1797.

[18] LI Yingsen, CHEN Ming, WANG Huanqing, et al. Finite-time adaptive dynamic surface fault-tolerant control for nonlinear systems[J]. Control Theory & Applications, 2022, 39(8): 1489-1496. (in Chinese)

[19] WANG L X, MENDEL J M. Fuzzy basis functions, universal approximation, and orthogonal least-squares learning[J]. IEEE Transactions on Neural Networks, 1992, 3(5): 807-814.

[20] LIU Yang, JING Yuanwei, LIU Xiaoping, et al. Survey on finite-time control for nonlinear systems[J]. Control Theory & Applications, 2020, 37(1): 1-12. (in Chinese)

[21] WANG H, CHEN B, LIN C, et al. Adaptive finite-time control for a class of uncertain high-order non-linear systems based on fuzzy approximation[J]. IET Control Theory & Applications, 2017, 11(5): 677-684.

[22] HAN Y Q, BIGGS J, CUI N G. Adaptive fault-tolerant control of spacecraft attitude dynamics with actuator failures[J]. Journal of Guidance Control and Dynamics, 2015, 38: 2033-2042.

Acknowledgements This work was supported in part by the National Key R&D Program of China (No. 2023YFB3307100), the National Natural Science Foundation of China (Nos. 62227814, 62203461, 62203365) and Shaanxi Provincial Science and Technology Innovation Team (No.2022TD-24).

Authors Ms. **WANG Kejun** received her B.S. degree from Department of Electrical Engineering and Automation and her M.S. degree from Department of Control Science and Engineering of Xi'an University of Posts and Telecommunications in 2020 and 2023, respectively. She is currently working toward the Ph.D. degree in control science and engineering, Rocket Force University of Engineering. Her current research interests include fault diagnosis, fault tolerant control, evidence theory, and multi-sensor data fusion.

Prof. **ZHOU Zhijie** received his B.Eng. and M.Eng. degrees from Rocket Force University of Engineering, Xi'an, China, in 2001 and 2004, respectively, and his Ph.D. degree from Tsinghua University, Beijing, China, in 2010, all in control science and management. He is currently a professor with the High-Tech Institute of Xi'an. His research interests include belief rule base, dynamic system modeling, hybrid quantitative and qualitative decision modeling, and fault prognosis and optimal maintenance of dynamic systems.

Author contributions Ms. **WANG Kejun** designed the study, complied the models, conducted the analysis, interpreted the results and wrote the manuscript. Prof. **ZHOU Zhijie** contributed to data and model components for the model. Dr. **FENG Zhichao** contributed to the discussion and background of the study. Dr. **YANG Ruohan** contributed to the discussion and background of the study. Dr. **HU Changhua** contributed to the discussion and background of the study. Dr. **XU Hui** contributed to the discussion and background of the study. All authors commented on the manuscript draft and approved the submission.

Competing interests The authors declare no competing interests.

(Production Editor: ZHANG Bei)

运载火箭执行器故障下自适应超螺旋滑模容错控制

王珂君[1],周志杰[1],冯志超[1],杨若涵[2],胡昌华[1],徐 慧[1]

(1.火箭军工程大学,西安 710025,中国;2.西北工业大学电子信息学院,西安 710129,中国)

摘要:针对存在执行器故障的运载火箭姿态指令跟踪问题,考虑到未知外部扰动、运载火箭燃料消耗和由贮箱晃动引起的转动惯量变化等不确定性,以及执行器故障和未建模动态导致的潜在系统模型变化,设计了一种基于自适应超扭曲滑模控制的容错控制律。该控制算法集成了超扭曲滑模控制、模糊逻辑控制和自适应控制方法。首先,选择超扭曲滑模面来缓解滑模控制固有的"抖振"现象,确保系统跟踪误差在有限时间内收敛到0。然后,基于该滑模面,利用模糊逻辑控制来逼近包含故障信息的未知系统函数。自适应参数用于逼近系统参数,并增强抗扰能力。利用李雅普诺夫方法证明了运载火箭姿态跟踪控制系统的稳定性和有限时间收敛性。数值仿真结果表明了所提出的自适应超扭曲滑模控制算法的有效性和鲁棒性。

关键词:运载火箭;执行器故障;超螺旋滑膜控制;容错控制;模糊逻辑控制